International Journal of Science and Research (IJSR)
ISSN: 2319-7064
SJIF (2019): 7.583

Wild Olive Tree Mapping Extent, Distribution and Basic Attributes of Wild Olive Trees in the Al-Baha Region, Saudi Arabia using Remote Sensing Technology

I. Enumerate, Extent, Distribution and Mapping

Abdullah Saleh Al-Ghamdi

Department of Biology, College of Sciences, Al-Baha University, P.O. Box 400, Al-Baha 31982, Kingdom of Saudi Arabia
Email: *abdullah.saleh.alghamdi[at]gmail.com*

Abstract: ***This study provides detailed information on the extent and distribution of wild olive trees in the Al-Baha region. The study area, concentrated along the Sarah Mountain, encompassed the districts of Al-Qura, Al-Mandaq, Al-Baha, the southern part of Baljurashi, and a small portion of the Qelwa, Mekhwa, and Al-Aqiq districts. This indicates that wild olive prefers high, foggy, mountainous conditions, which a previous study determined to be a medium to high vegetation density zone. The information extracted from high resolution Pleaides satellite images reveal that in the 1,991 km^2 of the area studied, only 817 km^2 (41%) has wild olive trees. The Al-Qura district has the highest percentage, with 46.0% covering 270 km^2, followed by Al-Mandaq, (44.3%, 150 km^2) and Al-Aqiq (41.6%, 69 km^2). However, the district with the lowest population of wild olive trees is Qelwa (29.5%, 24 km^2). The automated calculation of geographic information system (GIS) crown polygons transformed from Pleaides imagery classification enumerated a total of 717,894 wild olive trees at the study area or an average of 360 trees per km2. The Al-Mandaq district has the highest numbers, with 208,034 wild olive trees, followed by Baljurashi (178,801) and Al-Baha (161,802), whereas the Al-Qura, Qelwa, Mekhwa Al-Aqiq districts have the lowest number of wild olive trees. These results show that the Al-Mandaq district has the densest wild olive population, with 613 trees per km^2, followed by Al-Baha, which has 563 trees per km^2. Meanwhile, the Al-Aqiq district has the lowest wild olive tree density, with only 22 trees per km^2, followed by Al-Qura, which has 222 trees per km^2. From maps, it was observed that most wild-olive-dense areas are located at the north-eastern Al-Mandaq, south-western Baljurashi, and at the boundaries of Al-Baha. The overall accuracy of the interpretation was 91%, with producer accuracy and user accuracy being 93.7% and 88.3%, respectively. This information will be essential in identifying the landscape preference of the wild olive in the Al-Baha region***

Keywords: Wild olive, mapping extent, distribution, basic attributes, remote sensing, enumerate, mapping Al- Baha region, Saudi Arabia, Al-Mandaq, Baljurashi, Al-Qura, Al-Mekhwa, Al-Aqiq, Qelwah

1. Introduction

1.1 Wild Olive Tree

Olea oleaster, the wild olive, has been considered by various botanists to be a valid species and a subspecies–of the cultivated olive tree, *Olea europea*, which has multiple origins (Besnard and Berville, 2000) and was domesticated at various places during the fourth and third millennia BCE, in selections drawn from varying local populations (Besnard and Baradat, 2001).

Today, as a result of natural hybridization and the very ancient domestication and extensive cultivation of the olive throughout the Mediterranean Basin, wild-looking feral forms of olive, called "*oleasters*", constitute a complex of populations, potentially ranging from feral forms to the wild olive. (Lumaret, Ouazzani, Michaud, and Vivie, 2004).

The wild-olive is a tree of the maquis shrubland, which exists partly as a result of the long presence of mankind. The drought-tolerant sclerophyllous wild olive tree is believed to have originated in the Mediterranean Basin. It still provides the hardy and disease-resistant rootstock on which cultivated olive varieties are grafted (Breton *et al.*, 2006).

Meanwhile, wild olive is also reported to be native to North America an evergreen tree that reaches 20-feet with a10–15-foot spread. This small tree is very rarely found and is even reportedly close to extinction. The olive-like, white fruits it produces have a sweet flesh relished by birds and other wildlife and, although edible to humans, should not be eaten in quantities. However, in the United States of America, another olive tree species known as the Russian olive (*Elaeagnus angustifolia* L.) was considered an exotic invasive weed. This thorny shrub or tree originated from Southeastern Europe and Western Asia and was reported by Katz and Shafroth (2003) as intentionally introduced and planted in the United States for windbreaks, erosion control, wildlife habitat, and other horticultural purposes. This tree was then observed to be well adapted to semiarid and saline environments. Early in the 20th century, the Russian olive escaped cultivation and spread, particularly into the large moist riparian environments in the arid or semiarid regions of the western United States (Stannard *et al.,* 2002).

1.2 Mapping Wild Olive Tree Using Remote Sensing

Classifying and mapping vegetation is an important technical task for managing natural resources as vegetation provides a base for all living beings and plays an essential role in affecting global climate change, such as influencing terrestrial CO_2 (Xiao et al., 2004). Vegetation mapping also presents valuable information for understanding natural and man-made environments through quantifying vegetation cover from local to global scales at a given time point or over a continuous period. It is critical to the obtain current states of vegetation cover in order to initiate vegetation protection

and restoration programs (Egbert *et al*., 2002).

Traditional methods (such as field surveys, literature reviews, map interpretation, and collateral and ancillary data analysis) have been not been effective in acquiring mass vegetation covers because they are time consuming, date lagged, and often too expensive. Meanwhile, remote sensing offers a practical and economical means to study vegetation cover changes, especially over large areas (Langley et al., 2001; Nordberg and Evertson, 2003).

Because of the potential capacity for systematic observations at various scales, remote sensing technology covers possible data archives from the present to over several decades back. For this advantage, researchers and application specialists have made enormous efforts to delineate vegetation cover from local scale to global scale by applying remote sensing imagery. Since then, there have been numerous efforts taken regionally and nationally to map wild olives using remote sensing. An example is a pilot project initiated to develop a cost-effective method for mapping the Russian olive (*Elaeagnus angustifolia* L.), an invasive tree species, from scanned, large-scale aerial photographs. A study area was established along a riparian zone within a semiarid region of the Fishlake National Forest, located in central Utah.

Two scales of natural-color aerial photographs (1:4,000 and 1:12,000) were evaluated. Feature Analyst, an extension for ArcGIS and several image processing software packages, was used to map the invasive tree. Overall, Feature Analyst located the Russian olive (RO) throughout the imagery with a relatively high degree of accuracy. For the map derived from 1:4,000-scale photographs, the software correctly located the tree in 85% of all four-by-four meter transect cells where the Russian olive was actually present. However, smaller trees were sometimes missed and the size of trees and groups of trees were frequently underestimated. The map derived from the 1:4,000-scale photographs was only slightly more accurate than the map derived from the 1:12,000-scale photographs, suggesting that smaller-scale photography may be adequate for mapping the Russian olive (Hamilton *et al.,* 2006).

Another attempt was conducted at Australia to test the ability of remote sensing imagery to map olive groves and their attributes. Specifically, this attempt aimed to discriminate olives cultivars and to detect and interpret within-field spatial variability. Using high spatial resolution (2.8m) QuickBird multispectral imagery acquired over Yallamundi (southeast Queensland) on 24 December 2003, both visual interpretation and statistical (divergence) measures were employed to discriminate olive cultivars. Similarly, the detection and interpretation of within-field spatial variability was conducted on enhanced false colour composite imagery, and confirmed by the use of statistical methods. Results showed that the two olive varieties (i.e. Kalamata and Frantoio) can be visually differentiated and mapped on the enhanced image based on texture. The spectral signature plots showed little difference in the mean spectral reflectance values, indicating that the two varieties have a very low spectral separability (Apan, 2004).

In relation to olives, a study that used conventional-colour and colour-infrared aerial photographs and vegetation indices was conducted in Spain to determine variations in cover crop, bare soil, and tree areas in olive groves as affected by the season. They found that early summer was the most suitable time to distinguish between cover crops and olive trees. In addition, the study found that indices based on blue- and red-band reflectance values were suitable for cover crop and olive tree discrimination (Peña-Barragán *et al*., 2004).

2. The Study Area

The most effective way to map plant-species ranges in an area is by demarcating a general bioclimatic envelope within biogeographic regions where a species has been found. This study requires building a database of species that includes data on the distribution of species by geographic region, major habitat type, and elevation range (Price, 2004). Similarly, in this study, due to the large area and to save time, cost, and energy, the selected areas are only those with high probability of wild olive tree presence, as indicated by high (61.8 km^2) and medium (790.7 km^2) density vegetated area (Table 1) (Al-Ghamdi, 2020). However, it is also possible for wild olive trees to be found at nearby areas with lower vegetation density; hence, the study area was expanded to the northern part with low vegetation canopy density but not to the southern part because the southern part of Al-Mekhwah and Qelwa has a steep slope toward Tehama. This totaled the overall study area 1,991km^2 (Figure.2) (Al-Ghamdi, 2020), which is just 18.0% of the whole Al-Baha region. The study area covers almost all of A-Mandaq and Al-Baha districts, and 58.5% of the study area has low vegetation crown density.

Table 1: Study area extent according to districts

District		Study Area		Vegetation Crown Density					
Name	km^2	km^2	(%)	High	(%)	Med.	(%)	Low	(%)
Al-Qura	1,049	586	55.9	9	1.5	128	21.8	449	76.6
Al-Aqiq	3,667	165	4.5	0	0.0	21	12.7	144	87.3
Mandaq	361	339	94	23	6.8	247	72.9	69	20.4
Mekhwa	1,949	27	1.4	3	11.1	24	88.9	0	0.0
Al-Baha	298	287	96.4	17	5.9	106	36.9	164	57.1
Baljurashi	1,505	506	33.6	7	1.4	162	32.0	337	66.6
Qelwa	2,232	81	3.6	3	3.7	78	96.3	0	0.0
TOTAL	**11,060**	**1,991**	**18**	**62**	**3.1**	**766**	**38.5**	**1,163**	**58.4**

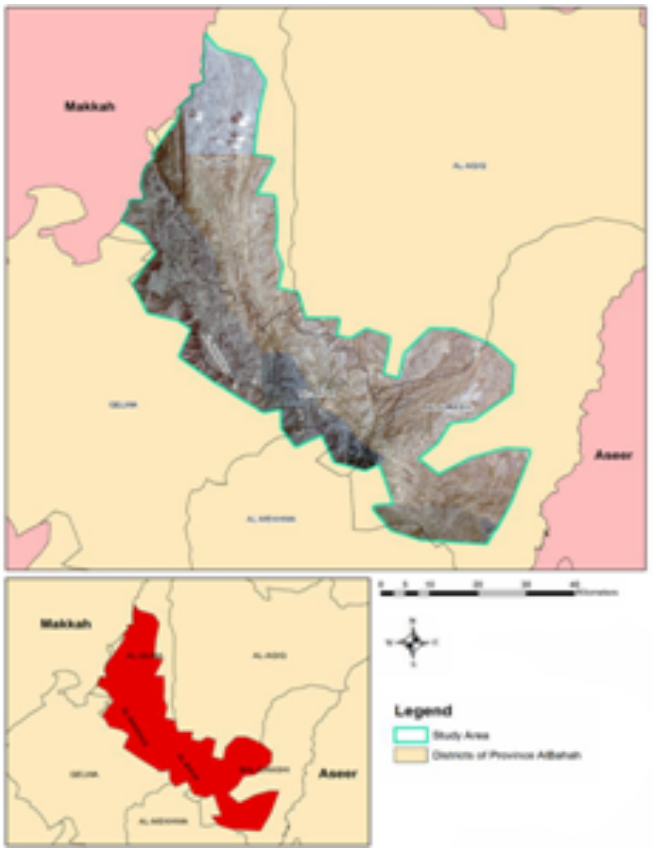

Figure 1: Satellite Pleaides image of study Area (in red)

2.1 Objectives

The main purpose of this study is to enumerate wild olive trees in the Al-Baha region and to produce high-quality, standardized maps of wild olive distribution to support a wide variety of resource assessment, management, and conservation. It can also be a guide for a standard national vegetation classification scheme and mapping protocols that will facilitate effective resource management by ensuring compatibility and widespread use of the information at multiple geographic scales throughout the Al-Baha federal and provincial agencies, Moreover, it will support researchers and decision makers in developing strategies and remedies. This wild olive inventory and mapping study involves purchasing high resolution satellite imagery and image processing methodology to classify and map the predetermined species of medium to high vegetation density across the Al-Baha region.

3. Materials And Methods

3.1 Materials and Data

In this study, due to mass area coverage and difficult terrain, satellite imagery was used as the main source for information extraction. The following software packages were used:

- ERDAS Imagine 2014: An image processing software.
- ArcGIS ver 10.3: A (GIS) software to analyze information extracted from satellite images.

The data obtained from the following was used in this study:

- Satellite image Pleaides dated 15 May 2016 (resolution 0.50 x 0.5 m)
- Shuttle Radar Topography Mission (SRTM) (elevation data extraction)
- Digital boundary of Al-Baha region and district

3.2 Method

Three main activities involved in this study are: data collection involving satellite data procurement, namely data collection, data analysis, and field work. The overall workflow of this study is shown in Figure 2. Satellite image LANDSAT-8, dated 15 May 2016, was used as the primary source for data extraction to identify vegetated areas in the Al-Baha region. Image LANDSAT-8 was downloaded from the USGS website and processed for Normalized Differential Vegetation Indices (NDVI) to demarcate areas with vegetation or chlorophyll. The detailed activities of the workflow are shown in Figure 2.

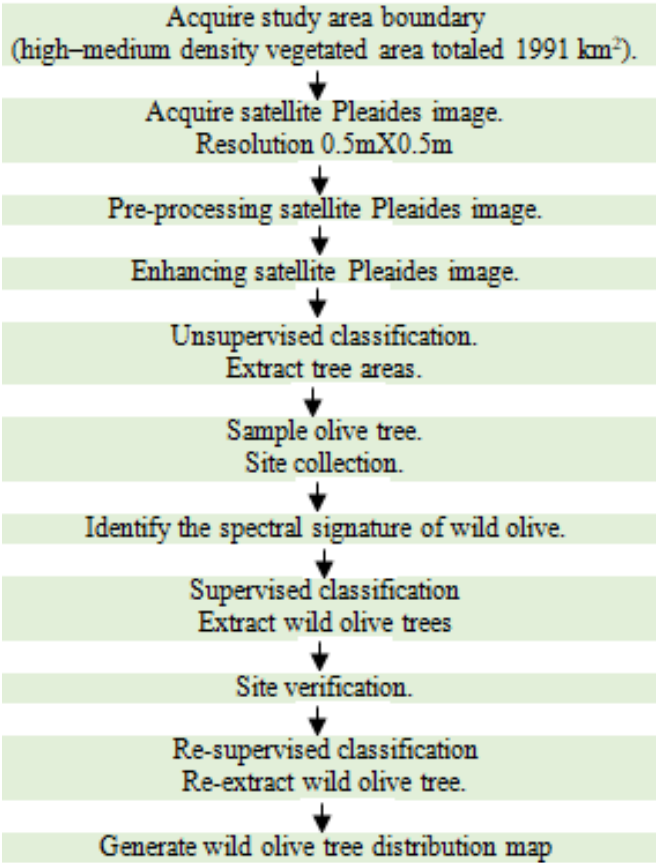

Figure 2: Workflow chart

3.3 Satellite Data Acquisition

The remote sensing data acquired from Pleaides satellite imagery (15 May, 2016) was purchased from ARIBUS Defence and Space through a local agent. The Pleiades images provide high-resolution imagery, from 0.5 meters to 2.0 meters, of earth's land surface and Polar Regions. A Pleiades swath covers 20 km at nadir, and the satellites' high agility facilitates the acquisition of a mosaic of images covering a larger area (up to 120km X 120km) in the same pass or stereoscopic images 300 km long.

The Pleiades bands are: panchromatic (450–830 nm), band 1

(blue 430–550 nm), band 2 (green 500–620 nm), band 3 (red 590–710 nm), band 4 (near infrared 740–940 nm).

3.4 Satellite Image Pre-processing

Image pre-processing is the process of making an image more interpretable for a particular application. It makes important features of raw, remotely sensed data more interpretable to the human eye. It includes data correction, such as radiometric correction, geometric correction, and so on.

ERDAS Imagine version 2014, a remote sensing software, was used to process the raw Pleaides data, including the radiometric correction, band combination, image enhancement, and other basic image processing system, for data analysis. ERDAS Imagine has raster graphics editor abilities designed by ERDAS for geospatial applications. It is aimed mainly at geospatial raster data processing and allows users to prepare, display, and enhance digital images for mapping use in GIS software (Hexagonspatial, 2016).

3.5 Image Enhancement and Filtering

The selection of a suitable band combination is essential for Pleaides as it makes enhanced images for visual interpretation. Removing the blurring and noise, increasing contrast, and revealing details are examples of its enhancement operations (Carl, 1996). There is no ideal level of image enhancement because the results are ultimately evaluated by humans, who make subjective judgments as to whether a given image enhancement is useful (Jensen, 2005). In this study, the images were enhanced using Histogram Equalize to contrast the different land use.

3.6 Spectral Signature

Spectral signature refers to the relationship between the wavelength (or frequency) of electromagnetic radiation (EMR) and the reflectance of the surface. The signature is affected by several things, including the material composition and structure. Some parts of the EMR spectrum, such as the microwave region, are more sensitive to surface structure than other regions. Spectral signature (or more often the sampled parts of it—bands of satellite imagery) infers information about the surface such as composition (e.g. vegetation and bare soil). These features are discriminable only if they have non-overlapped spectral signatures that can be normally viewed at the separability graph.

In this study, wild olive spectral signatures were extracted and compared from the prior image classification activity to ensure they were separable. The software specifically used was ENVI ver 5.4, which is another remote sensing software that combines advanced spectral image processing and geospatial analysis technology with a modern, user-friendly interface specifically used for more complicated images, such as high-resolution images, hyperspectral images, synthetic aperture radar (SAR) and light detection and ranging (LiDAR).

3.7 Ground Sample Collection

The ground sample collection activity is required to acquire several locations of wild olive trees at various district sites to be the 'training samples' for supervised classification. These locations were marked as wild olive tree coordinates on the image, and the spectral signature or digital number were recognized as a guide to search and demarcate other similar reflectance characteristics. In this project, about 30 points of wild olive trees were to run supervised classification. These points are shown in Figure 3.

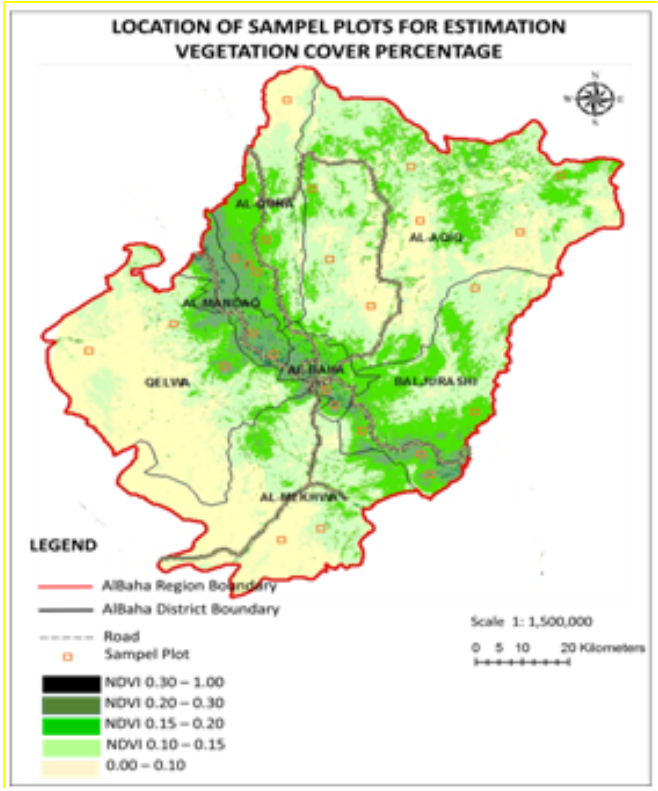

Figure 3: Location of plots for ground sample collection

3.8 Forest Inventory Design

In this project, the wild olive inventory was based on two major techniques:

- **Aerial inventory**: Using Pleaides satellite images, the whole study area was measured. The study area was divided to seven administrative districts: Al-Qura, Al-Aqiq, Al-Mandaq, Al-Baha, Baljurashi, Qehwa, and Al-Mekhwah. The attributes measured using aerial inventory are tree numbers and tree distributions.
- **Ground inventory sampling plot**: A certain number of plots statistically representing the whole area were randomly selected at the site and the measurement was taken 100% within the plot. The inventory process comprises designing the inventory, designing the forms of collecting the information, dividing the forest area into seven districts, describing the tree cover of each site, measuring all the trees and shrubs within each sampling plot, and analyzing the information obtained.

3.9 Accuracy Assessment

Accuracy assessment is the comparison of a classification

with ground truth data to evaluate how well the classification represents the real world. The step involved in accuracy assessment includes determining the number of samplings and the confidence building assessment and sampling design. In this project, the number of sampling follows the Krejcie and Morgan method, and the assessment follows the producer/consumer accuracy and plots selected based on random sampling techniques.

3.10 Determine the Number of Samples

The sample size of any study must be determined during the designing stage. However, before determining the size of the sample to be drawn from the population, a few factors must be taken into consideration. According to Salant and Dillman (1994), the size of the sample is determined by four factors:

(1) how much sampling error can be tolerated;
(2) population size;
(3) how varied the population is with respect to the characteristics of interest; and
(4) the smallest subgroup within the sample for which estimates are needed.

Using the above methods as a guideline, the following section uses Krejcie and Morgan (1970) and Cohen's statistical power analysis.

The estimation of sample size in research using Krejcie and Morgan is a commonly employed method. Krejcie and Morgan (1970) used the following formula to determine sampling size:
$S = X^2NP (1-P)/ d^2 (N-1) + X^2P(1-P)$
S = required sample size
X^2 = the table value of the chi-square for one degree of freedom at the desired confidence level
N = the population size
P = the population proportion (assumed to be .50 since this would provide the maximum sample size)
d = the degree of accuracy expressed as a proportion (.05)

In this study,
$S = X^2NP (1-P)/ d^2 (N-1) + X^2P(1-P)$
$=3.841 * 236,250 * 0.95 * (1-0.95) / 0.05 * 0.05 * (236,250-1)$
$= 41,963/575.18$
$=$ **73**

Therefore, a total of 73 plots of 50m x 50m were established in the study area.

3.11 Determining Sample Size

When assessing the accuracy of remotely sensed data, each sample point collected is expensive and therefore sample size must be kept to a minimum; yet, it is critical to maintain a large enough sample size so that any analysis performed is statistically valid. Because of the large number of pixels in a remotely sensed image, traditional thinking about sampling does not often apply (Congalton, 1991). Hence, this project followed the most common plot size established for the forest inventory of 50m x 50m, similarly applied by Lufty and Ismail (2012) for a recent vegetation inventory at Al-Baha.

3.12 Tree Enumeration

The enumeration of wild olive trees in the whole study area was determined digitally by ERDAS software upon supervised classification, where trees with similar reflectance as site-sample trees were interpreted as wild olive trees, and direct measurement at ground. Ground measurement was conducted during the month of October 2016 with 73 plots of 50m x 50m.

3.13 Error Matrix / Producer and Consumer Accuracy

The error matrix is the most common way of expressing the accuracy of remote sensing image classifications, such as land cover and species interpretation (Comber *et al.,* 2013). In the context of information extraction by image analysis, accuracy "measures the agreement between a standard assumed to be correct and a classified image of unknown quality." (Campbell, 2007) Precision defines the level of detail found within the classification. It is possible to increase the accuracy of a classification by decreasing the amount of detail or by generalizing it as broad classes rather than specific ones. The accuracy of image classification is most often reported as a percentage correct. An error matrix is a square array of numbers set out in rows and columns that express the number of sample units (i.e., pixels, clusters of pixels, or polygons) assigned to a particular category relative to the actual category as verified on the ground; this is shown in Table 3**.** The columns usually represent the reference data while the rows indicate the classification generated from the remotely sensed data. An error matrix is a very effective method of representing accuracy in that the accuracies of each category are plainly described along with both the errors of inclusion (commission errors) and errors of exclusion (omission errors) present in the classification (Congalton, 1991). The consumer's accuracy (CA) is computed using the number of correctly classified pixels to the total number of pixels assigned to a particular category. It takes errors of commission into account by telling the consumer that, for all areas identified as category X, a certain percentage is actually correct. The producer's accuracy (PA) informs the image analyst of the number of pixels correctly classified in a particular category as a percentage of the total number of pixels actually belonging to that category in the image. Producer's accuracy measures errors of omission.

3.14 Stratified Random Sampling

From the vegetation map generated from the first phase study, it was observed that the districts of Al-Baha have various vegetation density that is influenced by elevation. We may expect the measurement of wild olive trees to vary among the different districts. This has to be accounted for when we select a sample from the population so as to obtain a sample that is representative of the population. This can be achieved by stratified sampling. A stratified sample is obtained by taking samples from each stratum or sub-group of a population. When we sample a population with several strata, we generally require that the proportion of each stratum in the sample should be the same as in the

population.

Stratified sampling techniques are generally used when the population is heterogeneous or dissimilar, where certain homogeneous or similar sub-populations can be isolated (strata). Simple random sampling is most appropriate the sample is taken from a wholly homogeneous population. Some of the reasons for using stratified sampling rather than simple random sampling are:

a) The cost per observation in the survey may be reduced;
b) Estimates of the population parameters may be wanted for each sub-population;
c) Increased accuracy at a given cost.

As mentioned earlier, stratification was based on district boundaries and the numbers of plots are in proportion to district size. As the main portion of the study area is at a mountain with high elevation and rugged terrain and is not easily accessible, the plots selected have to consider accessibility and road proximity.

Trees bit further in the plot were remotely measured using laser range finder. In this project, verification was conducted on accuracy of the satellite-image-interpreted wild olive trees, which were classified 100% throughout the whole study area. We used the same 73 inventory plots earlier established to reduce time and energy.

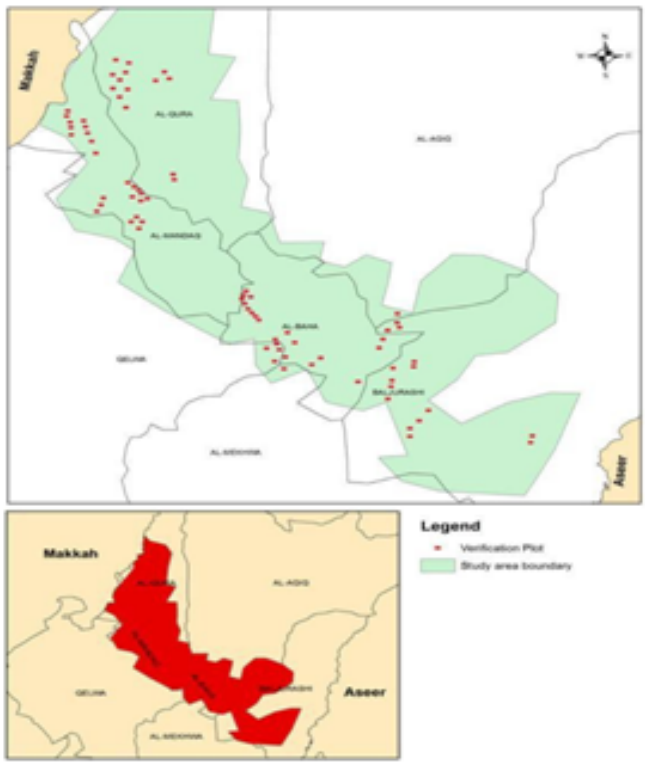

.

Figure 4: Location of plots for inventory and accuracy assessment.

4. Results

This report provides seven main results: (i) the extent and distribution of wild olive trees at Al-Baha by districts (ii) the extent and distribution of wild olive tree with their crown size (iii) the distribution map of wild olive trees with their clustering characteristics (iv) the distribution map of wild olive trees with their health status category (v) the distribution map of wild olive trees with neighbouring tree species (vi) the distribution map of wild olive trees with age category (vii) accuracy assessment results.

4.1 Extent and Distribution of Wild Olive Tree at Al-Baha

The information extracted from Pleaides satellite images reveal that from 1,991 ha of the study area, only 817 ha (41%) had wild olive trees. The Al-Qura district has the highest percentage of area with wild olive trees, with 46.0% covering 270 ha, followed by Al-Mandaq (44.3%, 150 ha) and Al-Aqiq (41.6%, 69 ha). The automated calculation of GIS crown polygons transformed from Pleaides image classification enumerated a total of 717,894 wild olive trees in the study area or an average of 360 trees per km^2. Table 3 shows that the Al-Mandaq district has the densest wild olive population, with 613 trees per km^2, followed by Al-Baha with 563 trees per km^2. Meanwhile, the Al-Aqiq district has the lowest wild olive tree density, with only 22 trees per km^2, followed by Al-Qura with 222 trees per km^2 (Table. 2). From the maps in Figures 5, 6, 7, 8, 9, 10, 11, 12 and 13, it can be observed that most areas with a dense wild olive population are located at the north-eastern Al-Mandaq, south-western Baljurashi, and the boundaries of Al-Baha.

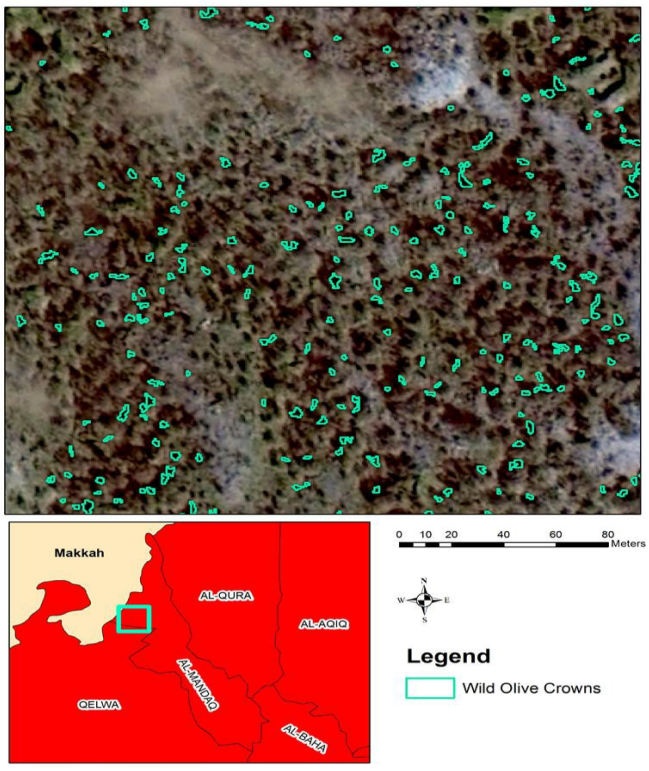

Figure 5: Satellite Pleaides Image classification identifying wild olive crowns

Table 2: Extent of wild olive trees at Al-Baha by districts

District	Study Area (km^2)	Area with wild olive tree		Number of wild olive tree	
		(km^2)	(%)	tree	Tree/ km^2
Al-Qura	586	270	46.0	129,903	222
Al-Aqiq	165	69	41.6	3,433	21
Mandaq	339	150	44.3	208,034	613
Mekhwa	27	10	38.9	11,851	444
Al-Baha	287	103	35.7	161,802	563
Baljurashi	506	192	37.9	178,801	353
Qelwa	81	24	29.5	24,070	297
TOTAL	1,991	817	41.0	717,894	360

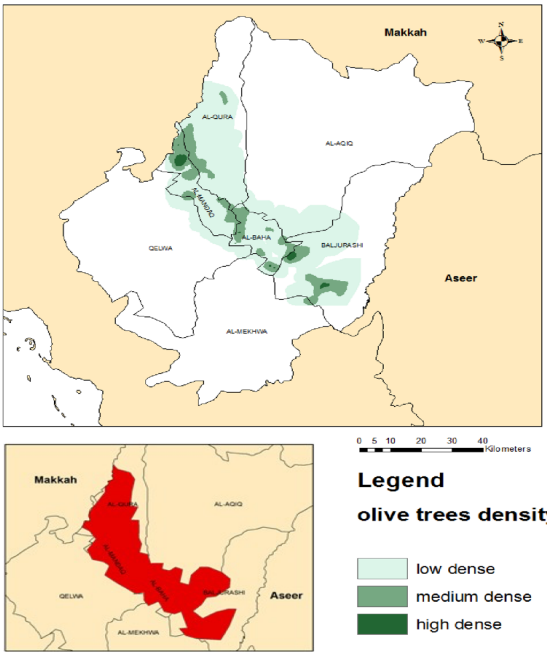

Figure 6: Distribution of wild olive canopy density in the Al-Baha region.

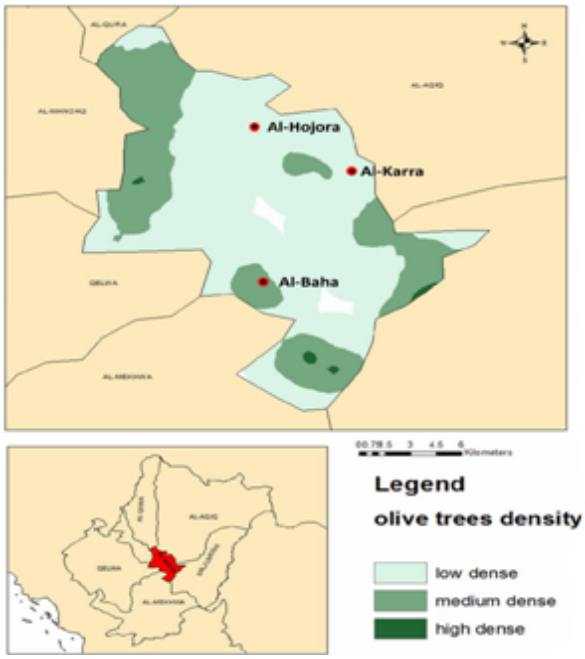

Figure 8: Distribution of wild olive canopy density in the Al-Baha district.

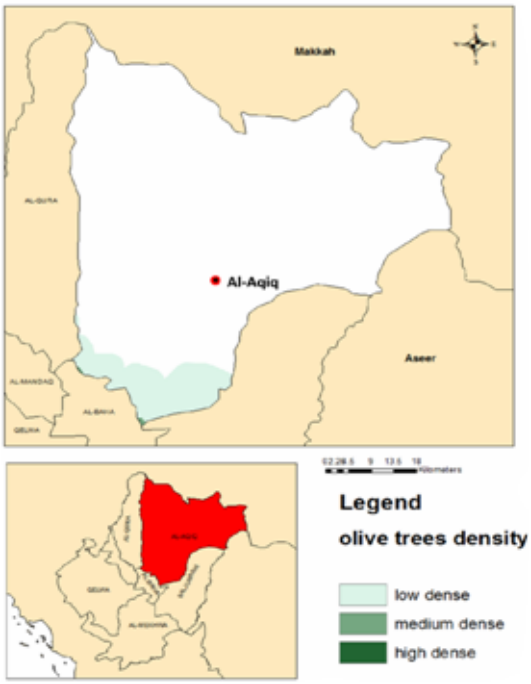

Figure 7: Distribution of wild olive canopy density in Al-Aqiq.

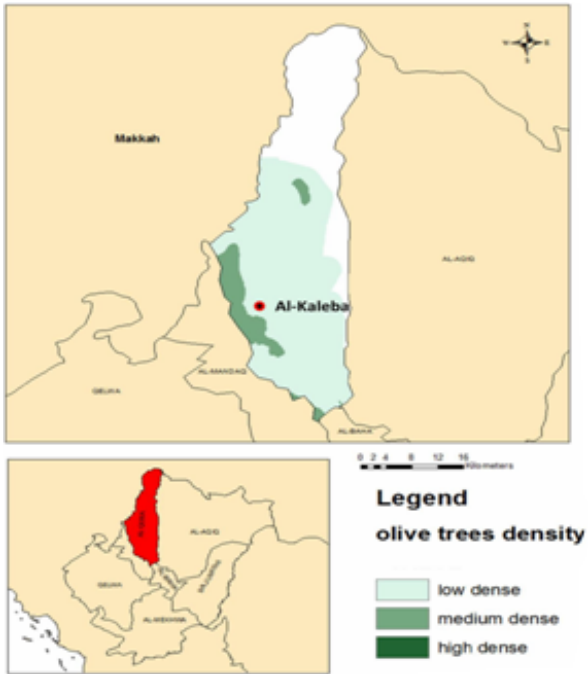

Figure 9: Distribution of wild olive canopy density in Al-Mandaq.

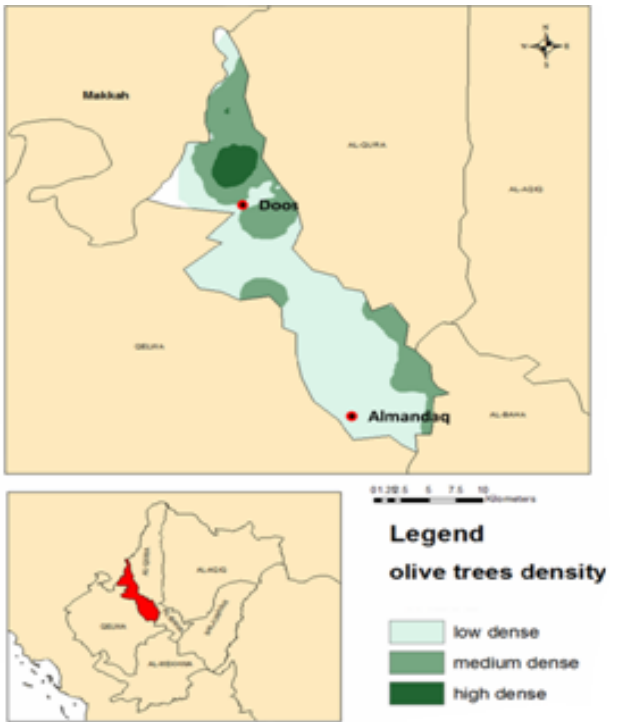

Figure 10: Distribution of wild olive canopy density in Al-Qura

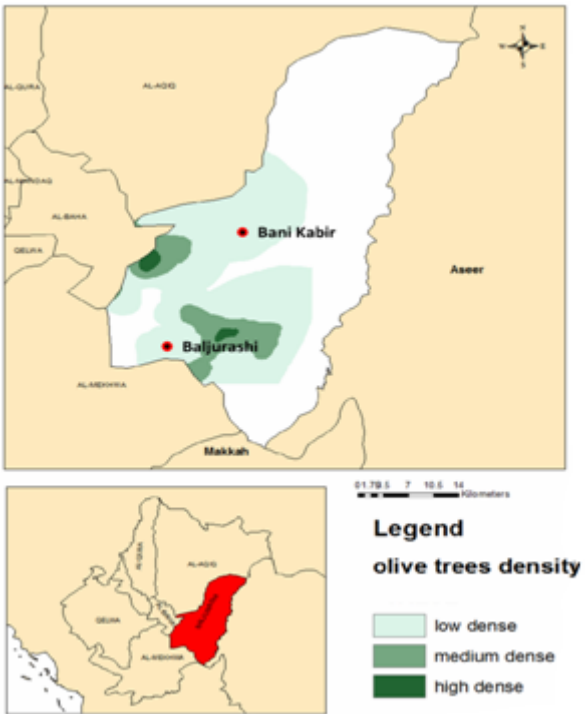

Figure 12: Distribution of wild olive Canopy density at Baljurashi

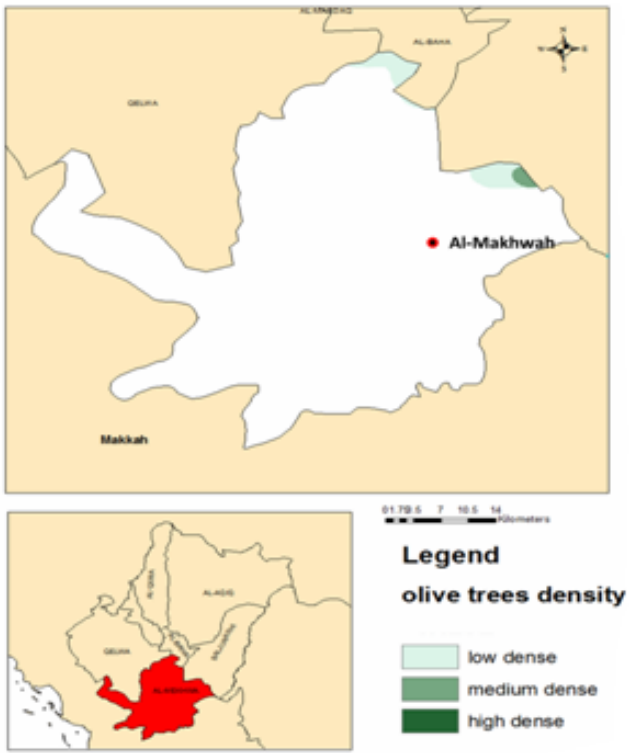

Figure 11: Distribution of wild olive canopy density at Al-Mekhwa

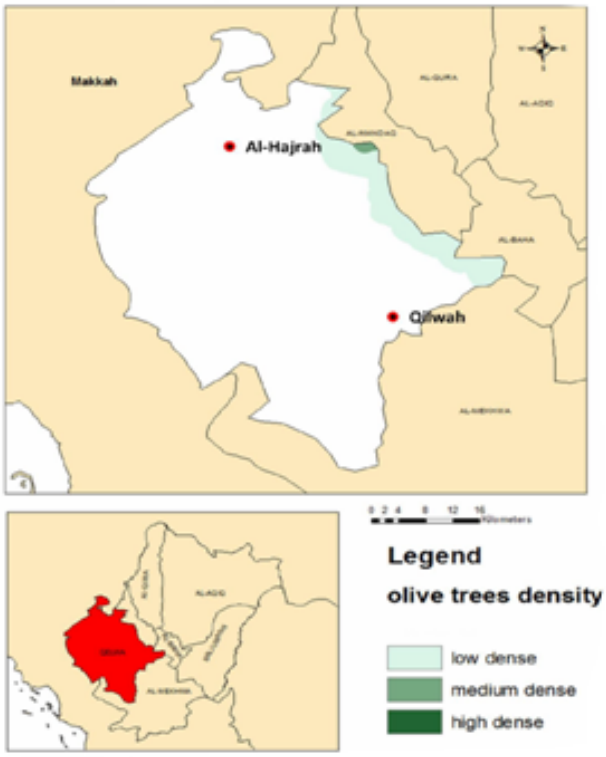

Figure 13: Distribution of wild olive canopy density at Qelwah.

Table 3: Accuracy assessment

		Tree numbers at site			
		Wild Olive	Acacia	Juniper	Total
Tree numbers at image	Wild Olive	414	22	33	469
	Acacia	12	289	22	323
	Juniper	16	21	337	374
	Total	442	332	392	1,166
Producers Accuracy: = 414/442 = 93.7%					
Users Accuracy: = 414/469 =88.3%					
Overall Accuracy: 1,040/1,166 =89.2%					

Accuracy Assessment

Accuracy assessments were conducted on 73 sampling plots of 50m x 50m at the site, randomly stratified based on districts. The results obtained shows that out of 469 wild olive trees interpreted on image, 414 trees were found true while there were 22 acacia and 33 juniper trees interpreted as wild olive. Thus, the accuracy of wild olive tree interpretation is 93.7% for producer accuracy and 88.3% for user accuracy. The overall accuracy of these interpretations is about 89.2%. Meanwhile, producer accuracy and user accuracy for acacia are 87.0% and 89.5%, respectively, and for juniper, they are 86.0% and 90.12%, respectively. The overall accuracy of the interpretation of species was 89.2%, with producer accuracy and user accuracy for wild olive interpretation being 93.7% and 88.3%, respectively

5. Discussion

The information extracted from high resolution Pleaides satellite imagery revealed that there are 717,894 wild olive trees (360 trees per km^2) in the study area, covering 1,991 km^2 and mostly found in the mountainous areas of the Al-Mandaq and Al-Baha districts. Researchers Al-Khulaidy (2013) and El-Juhany and M Aref (2012) referred to this region as the one with most plant diversity in Saudi Arabia. Previously, a similar study conducted by El-Juhany and M Aref (2012) at Al- Mandaq inventoried 147 tree species' trees per ha, whereas this study accounted for 613 wild olive trees per km^2. This indicates that wild olive is not the main species of vegetation in the Al-Baha region and many journals have reported juniper and acacia as the more abundant species.

6. Conclusion

This second-phase project has provided detailed information on the extent and distribution of wild olive trees in the Al-Baha region as well as the species attributes. The results obtained show that there are 717,894 wild olive trees (360 trees per km^2) in this 1,991-ha study area, concentrated along the Al-Sarawat mountain encompassing the districts Al-Qura, Al-Mandaq, Al- Baha, and the southern part of Baljurashi. This indicates that wild olive prefers high foggy mountainous conditions, which were previously predetermined, in the first-phase project, to have medium to high vegetation density.

Wild olive occurrence can be divided into three zones: (i) districts of Al-Mandaq and Al-Baha have higher wild olive density, younger trees, and smaller crown size, are highly clustered, and the wild olives are mostly neighbored by junipers. (ii) the districts of Al-Qura and Al-Baljurashi have lower wild olive density but have older trees and bigger crown size, are medium clustered, and the wild olives are mostly neighbored by acacias. (iii) the districts of Al-Aqiq, Qelwa, and Mekhwa have the least dense wild olives, younger trees, and smaller crown size, are lightly clustered, and the wild olives are mostly neighbored by junipers. However, Qelwa has more other species neighbouring the olives.

As the life-form distribution of plants growing in arid regions is closely related to its topography and landform (Aldhebiani and Howladar, 2013), this information will be essential to the third phase of the project: identifying the landscape preference of the wild olive in the Al-Baha Region.

7. Acknowledgements

This research was funded by the chair of Sheikh Said Ben Ali Alangari for olives research at Albaha University, Albaha, Saudi Arabia. The author also gratefully acknowledges the Deanship of Scientific Research (DSP) at Albaha University for their technical support and extends gratitude to Geoprecision Tech Sdn Bhd (GPT) and Universiti Putra Malaysia (UPM) for their technical help.

References

[1] Al-Ghamdi, A. S. (2020). Classifying and mapping of vegetated area in Al- Baha region, Saudi Arabia using remote sensing. I. Extent and distribution of ground vegetated cover categories. (Under publication).
[2] Al-Khulaidi A. A. (2013). Flora of Yemen. The Sustainable Natural Resource Management Project (SNRMP II), EPA and UNDP, Republic of Yemen (2013).
[3] Apan, A., Young, F. R., Phinn, S., Held, A., and Favier, J. (2004). Mapping olive varieties and within-field spatial variability using high resolution QuickBird imagery. In Proceedings of 12th Australasian Remote Sensing and Photogrammetry Conference, Spatial Science Institute. (12th Australasian Remote Sensing and Photogrammetry Conference, 18-22 October 2004, Fremantle, Australia.)
[4] Besnard, G. B. (2000). Genetic relationships in the olive

(*Olea europaea* L. reflect multilocal selection of cultivars, *Theoretical and Applied Genetics*.

[5] Besnard, G., and Berville, A. (2000). Multiple origins for Mediterranean olive (*Olea europaea* L. ssp. *europaea*) DNA polymorphisms, *Comates Rendus de l'Académie des Sciences* (online abstract).

[6] Breton, C., Tersac, M. et al. (2006). Genetic diversity and gene flow between the wild olive (oleaster, *Olea europaea* L.) and the olive: Several Plio-Pleistocene refuge zones in the Mediterranean basin, *Journal of Biogeography*.

[7] Rapp, C. S. (1996). Image processing and image enhancement, East Tennessee University, Johnson City, Texas.

[8] Campbell, J. B. (2007). Introduction to remote sensing (4th ed.). London: Taylor and Francis.

[9] Comber A., Fisher P., Brunsdon C., Khmag A. (2012). Spatial analysis of remote sensing image classification accuracy, *Remote Sensing of Environment* 127:237–246.

[10] Comber A., Linda S., Steffen F., van der Velde, M., Christoph P., and Giles F. (2013). Using control data to determine the reliability of volunteered geographic information about land cover. *International Journal of Applied Earth Observation and Geoinformation* 23, 37–48.

[11] Congalton R. G. (1991). A review of assessing the accuracy of classifications of remotely sensed data, remote sens. *Environ*. 37:35–46.

[12] Congalton, R. G. (1991). A comparison of sampling schemes used in generating error nmtrices for assessing the accuracy of maps generated from remotely sensed data, *Photogramnt. Eng. Remote Sens*. 54(5):593–600.

[13] Egbert S. L., Park S., Price K.P. et al. (2002) Using conservation reserve program maps derived from satellite imagery to characterize landscape structure. *Comput Electron Agric* 37:141–56.

[14] El-Juhany, L. I. and Aref, I. M. (2012). The present status of the natural forests in the southwestern Saudi Arabia: 1-Taif Forests. World, *Applied Sciences Journal*, 19(10): 1462–1474.

[15] El-Juhany, L. I., and Aref I. M. (2012) The present status of the natural forests in the southwestern Saudi Arabia 2-baha forests, world, *Applied Sciences Journal* 20(2): 271–281, ISSN 1818-4952.

[16] Hamilton, R., Megown, K., Lachowski, H., and Campbell, R. (2006). Mapping Russian olive: using remote sensing to map an invasive tree. RSAC-0087-RPT1. Salt Lake City, UT: U.S. Department of Agriculture Forest Service, Remote Sensing Application Center. 7 p.

[17] Hexagonspatial (2016), Erdas Imagine, Website: http :// www. hexagongeospatial. Com / products / producer suite/ erdas-imagine.

[18] Jensen, J. R. (2005), Introductory Digital Image Processing (3rd Edition), Prantice Hall.

[19] Katz, G. L. Shafroth, P. B. (2003). Biology, ecology and management of Elaeagnus angustifolia L. (Russian olive) in western North America. Wetlands 23:763–777.

[20] Krejcie, R. V., and Morgan, D. W. (1970). Determining sample size for research activities. *Educational and Psychological Measurement*, 30, 607–610.

[21] Langley S. K., Cheshire H. M., and Humes K. S. (2001). A comparison of single date and multitemporal satellite image classifications in a semi-arid grassland, *J Arid Environ* 49:401–11.

[22] Lumaret, R., Ouazzani, N., Michaud, H., and Vivie, G. (2004). Allozyme variation of oleaster population (wild olive tree) (*Olea europaea* L.) in The Mediterranean Basin) *Heredity*.

[23] Nordberg M.L., and Evertson J. (2003) Vegetation index differencing and linear regression for change detection in a Swedish mountain range using Landsat TM and ETM+ imagery. Land *Degradation & Development* 16:139–149.

[24] Peña-Barragán, J. M., Jurado-Expósito, M., López-Granados, F., Atenciano, S., Sánchez-de la Orden, M., García-Ferrer, A. and García-Torres, L. (2004). Assessing land-use in olive groves from aerial photographs, Agriculture, *Ecosystems & Environment*, 103(1): 117–122.

[25] Price, J. P. (2004). Floristic biogeography of the Hawaiian Islands-Influences of area, environment and paleogeography: *Journal of Biogeography*, v. 31, p. 487–500.

[26] Salant, P., and Dillman, D. A. (1994). How to conduct your own survey. New York: John Wiley & Sons, Inc.

[27] Stannard, M. Ogle, D. Holzworth, L. Scianna, J., and Sunleaf, E. (2002). History, biology, ecology, suppression and revegetation of Russian-olive sites (Elaeagnus angustifolia L.). Plant Materials Technical Note No. 47. Boise, ID. U.S. Department of Agriculture, Natural Resources Conservation Service, 14 p.

[28] Xiao X. M., Zhang Q., Braswell B. et al. (2004) Modeling gross primary production of temperate deciduous broadleaf forest using satellite images and climate data. *Remote Sens Environ* 1:256–70.